Microwave induced MIP synthesis: comparative analysis of thermal and microwave induced polymerisation of caffeine imprinted polymers

Nicholas W. Turner,[a] Clovia I. Holdsworth,[a] Scott W. Donne,[a] Adam McCluskey[a] and Michael C. Bowyer*[ab]

Received (in Victoria, Australia) 6th October 2009, Accepted 1st December 2009
First published as an Advance Article on the web 5th February 2010
DOI: 10.1039/b9nj00538b

Caffeine templated molecularly imprinted polymers (MIPs) have been prepared using identical polymer formulations by thermal and microwave induced initiation, and the binding performance of the systems compared using solid phase extraction (SPE). While the binding capacity of $MIP_{(Microwave)}$ was found to be lower than $MIP_{(Thermal)}$, $MIP_{(Microwave)}$ recorded a higher imprinting factor (IF) due to comparatively low levels of non-specific binding. Selectivity against theophylline in cross-reactivity studies was also found to be greater for $MIP_{(Microwave)}$. While large time savings are achievable through the use of microwave irradiation conditions, physical analysis of the polymers (surface area analysis, thermal gravimetric analysis and differential scanning calorimetry) reveals that the different polymerisation methods lead to differences in both polymer structure and performance.

Introduction

Molecular imprinting imparts the level of affinity and selectivity observed by biological recognition motifs (such as antibodies) into robust, reusable polymeric materials.[1–3] Molecularly imprinted polymers (MIPs) are commonly based on the use of highly cross-linked acrylate polymers, however a variety of other materials have been successfully utilised to demonstrate the technique. MIP synthesis is most commonly conducted *via* a ''non-covalent'' approach in which specific recognition is introduced by complementarities of interaction (H-bonding, salt bridges, van der Waals and π–π stacking interactions). Effective non-covalent imprinting requires that the template (analyte) and functional monomer associate in a solvent (known as a porogen) in the presence of a cross-linking agent and a free-radical initiator prior to polymerisation by either thermal or photochemical means. This affords a polymer monolith that is subsequently ground and sieved to obtain particles of suitable size from which the template is removed by exhaustive extraction, leaving tailored binding cavities capable of rebinding the template (Fig. 1).[4]

The clear benefits of such robust and highly specific systems have led to a rise in interest over the past decade or so, resulting in significant refining of the imprinting technique, with multiple nuances aimed at increasing both capacity and specificity, while simultaneously reducing laborious production and evaluation periods.[1] Examples include: rational design of polymers using a combination of molecular modelling and NMR titration to select optimal functional monomers and to optimise template and functional monomer ratios;[5–8] development of novel monomers specific for task;[9] creation of uniform particles by precipitation polymerisation,[10,11] emulsion polymerisation[12,13] and core shell polymerisation,[14–16] stimuli-responsive imprints,[17] and development of rapid screening techniques.[18] Common methods of rebinding analysis of bulk materials include batch binding (or solution depletion) and solid phase extraction (SPE).[19–22] While the former enables equilibration, hence a more accurate representation of polymer performance, it consumes significant amounts of laboratory time. By contrast, SPE is conducted over a short timeframe (seconds), yields similarly representative results and is portable, which has led to some of the first commercial MIP products based on this technology.[23]

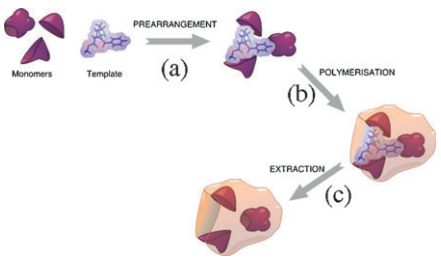

Fig. 1 Development of molecular imprinted polymers. (a) Pre-association of template with functional monomers; (b) polymerisation results in cavity formation; and (c) template removal to leave template specific cavity.

While modifications in methodology are capable of eliciting dramatic reductions in polymerisation and analysis times, changes to the polymer reaction conditions can have a significant effect on performance and production. For example, the choice of solvation conditions during polymerisation can exert significant influence over the performance of the resultant polymer. Bunte *et al.* created polymers for 2,4,6-trinitrotoluene in three different solvents (acetonitrile, chloroform and dimethylformamide), with each giving different performance

[a] *Centre for Organic Electronics, Chemistry Building, School of Environmental and Life Sciences, University of Newcastle, Callaghan, NSW 2308, Australia*
[b] *Discipline of Applied Sciences, School of Environmental and Life Sciences, University of Newcastle, Ourimbah, NSW 2258, Australia. E-mail: michael.bowyer@newcastle.edu.au; Fax: +61 2434 84145; Tel: +61 2434 8119*

with respect to rebinding of the template.[24] Our own research using room temperature ionic liquids as porogens has shown significant improvements in performance over traditional organic solvents,[25,26] with increased specificity and capacity and a reduction in analysis time with cocaine-based MIPs.

Despite these refinements, the core approach to polymerisation has remained largely consistent, involving thermal or UV decomposition of radical initiators, such as 2,2-azobis-(isobutyronitrile) (AIBN) and 1,1′-azobis(cyclohexanecarbonitrile) (ABCN). By far, the most common method is that of thermally initiated imprinting, where the pre-polymer mix is heated to 60 °C for a period of 18–24 h.[26,27] The downside to this approach is that the reactants are exposed to excess thermal energy, which raises the system's internal energy and impacts on the formation of the monomer–template complex, which is under thermodynamic control.[28] Piletsky *et al.* demonstrated that MIPs prepared by thermal methods (heating at 60 °C in an oil bath or oven) can produce significantly higher core temperatures inside the reaction vessel.[29] It was shown that reducing the reaction temperature improved the performance of the imprinted system. Photochemical initiation is now widely applied in MIP synthesis as it allows for the polymerisation process to be carried out at much lower temperatures with generally improved results.[25,29]

The use of laboratory (monomodal) microwave reactors is now routine in synthetic chemistry, resulting from the fact that microwave irradiation facilitates homogeneous and rapid heat transfer through the reaction mixture.[30] While the thermal benefits (rapid and even heating) of microwave heating are obvious, controversial non-thermal microwave effects are sometimes observed.[31] Recently, polymer synthesis by microwave irradiation has become popular, with most types of polymerisations, including step growth, free and controlled radical and ring opening polymerisations possible as well as modification and curing reactions.[32–35] Benefits include rapid synthesis, decreased side reactions (which increase product purity), higher yields with greater monomer conversion and the ability to use "green" solvent systems.[33,36] Differences in physical properties between microwave and thermally produced polymers have been noted, with higher molecular weights and lower polydispersity observed in microwave free-radical polymerisation systems.[37]

Recently, Zhang *et al.* utilised microwave heating to prepare atrazine imprinted methacrylic acid (MAA) beads housing a magnetic core, by suspension polymerisation.[38] Preparation time was shortened by 90% (2 h. *cf.* 24 h.) compared with traditional preparation methods and an improved polymer performance was observed (an imprinting factor of 4.7 for microwave *vs.* 2.7 for conventional heating). Significant levels of cross-reactivity were however observed.

Concurrent to this research, our research group has been pursuing similar work using the classical imprinting model of caffeine/theophylline (Fig. 2).[11,15,22,39] In this paper, we present findings demonstrating that microwave induced polymerisation performed under a further reduced time frame (14 min) leads to differences in morphology and structure between the MIP and its non-imprinted control polymer (NIP) that affect relative rebinding performance.

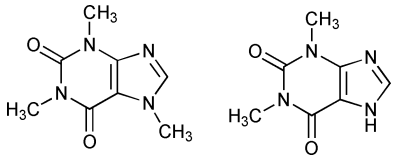

Fig. 2 Caffeine (left) and theophylline (right).

Results and discussion

A concentration-dependent target rebinding study (0–2.5 mmol) was undertaken using SPE to compare the binding efficacy of the thermal and microwave polymers. Both MIPs were found to selectively adsorb significantly greater quantities of caffeine than their respective control polymers (Fig. 3).

The binding capacity of $MIP_{(Thermal)}$ exceeded that of $MIP_{(Microwave)}$ by between 30 and 50% across the concentration range examined, suggesting that the short reaction time of the microwave polymer results in fewer accessible binding sites being formed. Surprisingly, differences were also observed in the rebinding behaviour of the non-imprinted control polymers. While caffeine rebinding was found to be linearly concentration dependent for both $NIP_{(Thermal)}$ and $NIP_{(Microwave)}$ across the concentration range tested, binding to $NIP_{(Microwave)}$ was quantitatively lower, suggesting that the choice of polymerisation method impacts on the microstructure of the resultant polymer.

Average imprint factors (IF) of 2 and 3.5 were determined for $MIP_{(Thermal)}$ and $MIP_{(Microwave)}$, respectively. The $MIP_{(Thermal)}$ value was consistent with previous literature reports for thermally produced caffeine imprinted polymers,[13–15] while the higher IF value for $MIP_{(Microwave)}$ was in general agreement with the findings of Zhang.[38] However, the apparent improvement of the IF of $MIP_{(Microwave)}$ provides a pertinent reminder of the caution that must be exercised when quoting ratio-based parameters, as the higher numeric value is a product of non-selective binding in $NIP_{(Microwave)}$ rather than increased imprinting efficiency in $MIP_{(Microwave)}$.

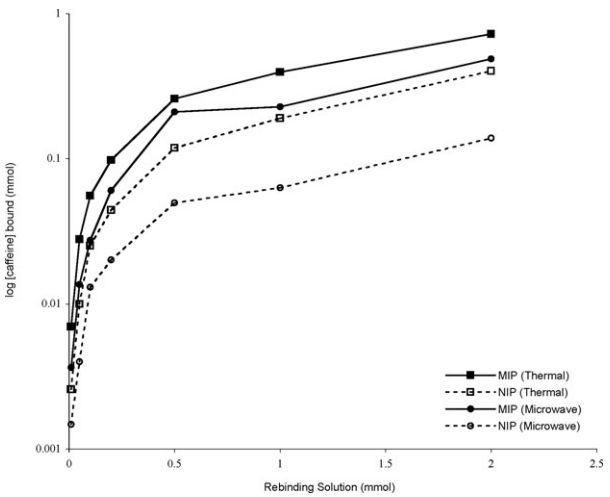

Fig. 3 Solid phase extraction rebinding data (100 mg of polymer) from 1 mL of caffeine solution: (a) thermal polymers (squares); and (b) microwave polymers (circles). Solid lines = MIP, broken lines = NIP. $n = 3$ for each point.

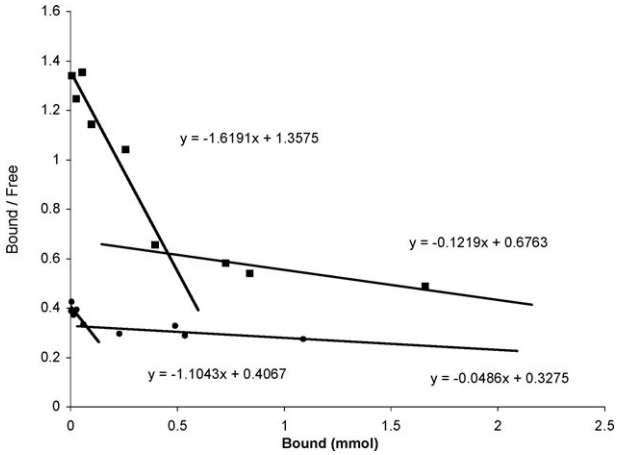

Fig. 4 Scatchard plots for rebinding of caffeine to $MIP_{(Thermal)}$ (■) and $MIP_{(Microwave)}$ (●) determined by SPE.

Scatchard analysis, (Fig. 4) was undertaken to further probe the nature of the binding characteristics of the thermal and microwave MIPs. Both polymers displayed a two-component profile consistent with the presence of high and low affinity binding sites. The $MIP_{(Microwave)}$ curve was proximally located below that of $MIP_{(Thermal)}$ for all concentrations examined, with the $MIP_{(Microwave)}$ breakpoint occurring closer to the graph origin, indicating that high affinity binding sites saturate at a lower analyte concentration.

Key parameters extracted from the curves (Table 1) quantitatively reinforce the differences between the two MIPs. Significantly higher K_D values for both the high and low affinity binding sites of $MIP_{(Microwave)}$ suggest that microwave irradiation promotes the formation of comparatively fewer well defined binding cavities. However, the ratio of low and high affinity K_D values ($K_{D(low)}/K_{D(high)}$ differs significantly between the MIPs, being higher for $MIP_{(Microwave)}$, suggesting that greater discrimination in binding character exists between the two domains. Microwave promoted polymerisation also appears to affect the distribution of binding sites, with the relative ratio of low to high affinity binding sites (N_{low}/N_{high}) being five-fold greater compared to $MIP_{(Thermal)}$. In absolute terms, the population of high affinity sites present on $MIP_{(Microwave)}$ is less than half that of $MIP_{(Thermal)}$, suggesting that the rapid polymerisation conditions may be akin to a "snap freezing" of the pre-polymer mix, limiting the thermally driven template–functional monomer equilibration processes known to be required to form high affinity binding sites.[28]

Table 1 Equilibrium data and binding site populations extracted from Scatchard plots using the plot formula of $([B]/[F]) = -(1/K_D[B]) + (N/K_D)$ where B = bound caffeine, F = free caffeine, K_D = dissociation constant and N = total recognition cavity concentration (maximum cavity binding)

Polymer	K_D/M	$(K_{D(low)}/K_{D(high)}$	N/mol g^{-1}	$(N_{(low)}/N_{(high)}$
$MIP_{(Thermal)}$ high affinity	0.618	13.2	8.39×10^{-3}	3.67
$MIP_{(Thermal)}$ low affinity	8.20		30.8×10^{-3}	
$MIP_{(Microwave)}$ high affinity	0.906	22.7	3.68×10^{-3}	18.3
$MIP_{(Microwave)}$ low affinity	20.6		67.4×10^{-3}	

Cross-reactivity studies (conducted under identical conditions to the caffeine study) were then performed using theophylline to evaluate cavity selectivity. Both polymer sets were observed to bind greater quantities of theophylline relative to caffeine (Fig. 5a,b *cf*. Fig. 3). Modest theophylline selectivity was observed for both $MIP_{(Thermal)}$ and $MIP_{(Microwave)}$, with uptake again being quantitatively higher for the thermal system.

All polymers bound considerably greater quantities of theophylline relative to caffeine (Fig. 5a,b). Modest theophylline selectivity was observed for both $MIP_{(Thermal)}$ and $MIP_{(Microwave)}$, with uptake again being quantitatively higher for the thermal system. The higher binding affinity displayed towards theophylline by both polymers was not unexpected given the smaller relative size and greater hydrogen bonding capability of the molecule. While selectivity compared with caffeine was expectedly poor, greater relative differential binding (the difference between MIP and NIP for each system) was again observed for the microwave produced polymers.

This point is illustrated more clearly when the imprinting factors for the two sets of experiments are directly compared (Fig. 6). $MIP_{(Microwave)}$ exhibits superior relative binding

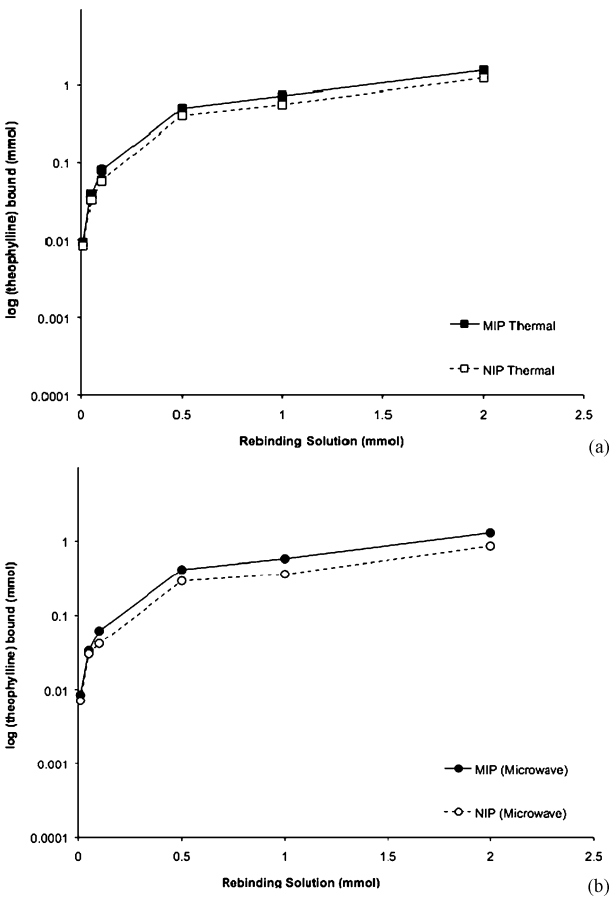

Fig. 5 Solid phase extraction rebinding data (100 mg of polymer) from 1 mL of theophylline solution: (a) thermal polymers (squares); and (b) microwave polymers (circles). Solid lines = MIP, broken lines = NIP. n = 3 for each point.

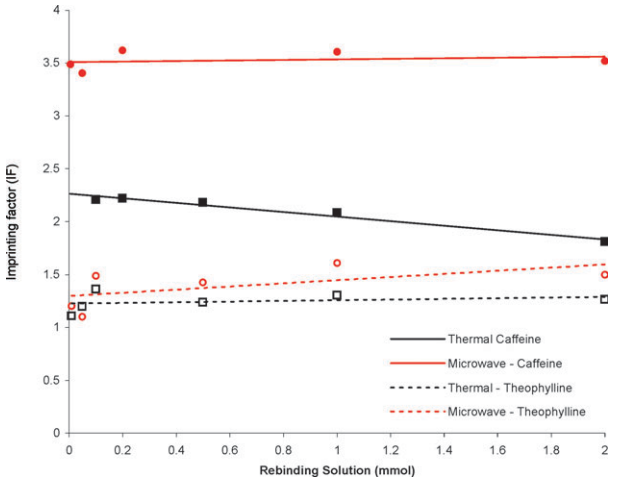

Fig. 6 Imprinting factors of analytes binding to caffeine templated polymers plotted *vs.* concentration of rebinding solution, calculated from data presented in Fig. 3 and 5. Solid lines = caffeine, broken lines = theophylline. Red = microwave, black = thermal for both systems. $n = 3$ for each point.

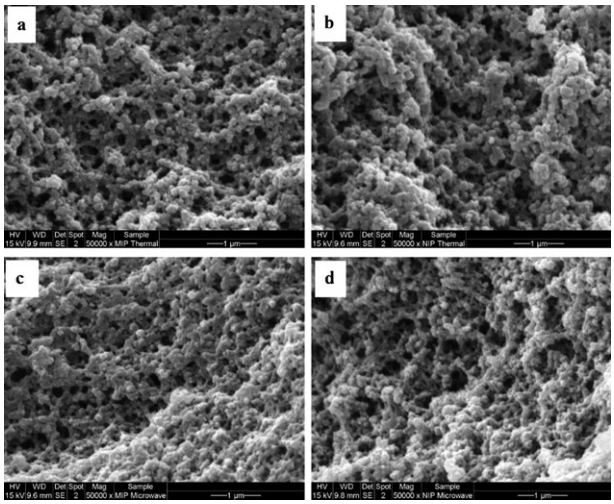

Fig. 7 SEM micrographs of the polymers (50 000× magnification). (a) $MIP_{(Thermal)}$; (b) $NIP_{(Thermal)}$; (c) $MIP_{(Microwave)}$; and (d) $NIP_{(Microwave)}$.

across the entire concentration range investigated. The differential in imprinting factor for caffeine relative to theophylline is large in the case of $MIP_{(Microwave)}$ (3.5 *cf.* 1.25) but only modest for $MIP_{(Thermal)}$ (~2 *cf.* 1.25), suggesting that while $MIP_{(Microwave)}$ possesses lower binding capacity as a result of a smaller number of well defined binding sites, comparative recognition is improved through reduced levels of non-specific binding.

Zeta potential measurements were recorded for each polymer (data not shown) to allow for a comparison of surface charge distribution. Average charge magnitude was found to be greater in both non-imprinted polymers relative to their imprinted counterparts, a result we attribute to the absence of imprint cavities, resulting in a greater proportion of functional monomer groups being located at the NIP surface. Analysis of variance (ANOVA) and post-hoc analysis of the data revealed significant differences in the average surface charge of all polymers except $MIP_{(Microwave)}$ and $MIP_{(Thermal)}$. While the results clearly communicate the importance of the template in influencing the physicochemical properties of the resultant polymer, they also appear to reinforce mode of polymerisation as a secondary determinant of polymer structure for both imprinted and non-imprinted polymers.

An assessment of the physical properties of the polymers was then undertaken to attempt to elucidate factors that might adequately explain the differences in binding behaviour. SEM analysis (Fig. 7) of the thermal and microwave MIPs and NIPs shows no obvious difference in gross morphology.

However, determination of polymer surface area *via* gas adsorption analysis revealed significant differences between all polymers (Table 2).[40] Two observations are immediately drawn from the data; (i) the surface areas of the thermally produced MIP and NIP exceeds that of their microwave counterparts, (ii) the surface area of $MIP_{(Microwave)}$ and $MIP_{(Thermal)}$ are greater than their respective NIPs.

The fall in surface area between the thermal and microwave polymerisation processes is significant, being 61% in the case of the MIPs and 35% in the case of the NIPs, We attribute the difference to be primarily an artifact of the longer reaction time associated with thermal polymerisation, which magnifies the influence of the porogen during chain growth and cross-linking, leading to greater porosity. The higher surface area of the MIPs under both microwave and thermal polymerisation conditions suggests that the template is also a surface area determinant, a fact that is further reinforced when surface areas of the MIP/NIP couples are analysed. Again, the greatest relative surface area decrease (from MIP to NIP) occurs under thermal polymerisation conditions (46%), as against a modest 10% change for microwave polymerisation. With conditions being identical in these comparisons, surface area differences can be directly correlated to template induced cavity formation. We have previously noted template effects on polymer architecture in the preparation of phase inverted molecularly imprinted films for TNT.[41]

Table 2 BET surface area of the polymers measured by nitrogen adsorption[40]

Polymer	BET/m^2 g^{-1}	Polymer	BET/m^2 g^{-1}
$MIP_{(Thermal)}$	399	$NIP_{(Thermal)}$	214
$MIP_{(Microwave)}$	154	$NIP_{(Microwave)}$	140

Further analysis of polymer porosity using density functional theory (DFT) (Fig. 8) supports this tenet, revealing that while all polymers possess similar macroporosity (observed in the SEM), distinct differences occur at the mesopore level, accounting for the observed variations in total surface area. Comparing $MIP_{(Thermal)}$ and $NIP_{(Thermal)}$, we note a proportionately greater presence of macropores in the 100–300 Å diameter range and a significant mesopore population centred around 40 Å. This effect, while also present in the microwave polymer couple, is much less pronounced in the mesopore range. Since the only difference between the MIP and NIP formulations is the presence or absence of template, it can be surmised that the template is responsible for the observed differences. The caffeine molecule is approximately 7 Å in size; therefore we speculate that these are vacated

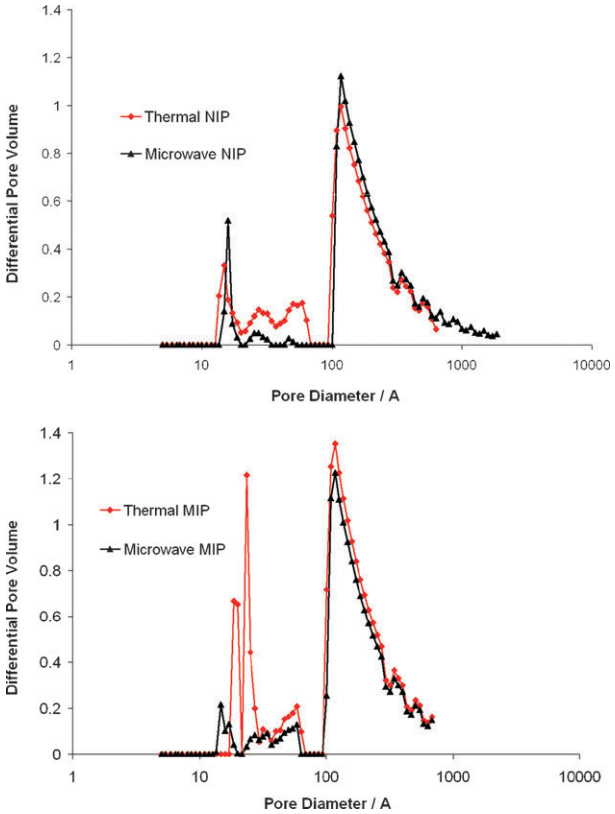

Fig. 8 Density functional theory pore size analysis using nitrogen adsorption. Top: non-imprinted polymers. Bottom: molecularly imprinted polymers. Red: MIP/NIP$_{(Thermal)}$, black: MIP/NIP$_{(Microwave)}$.

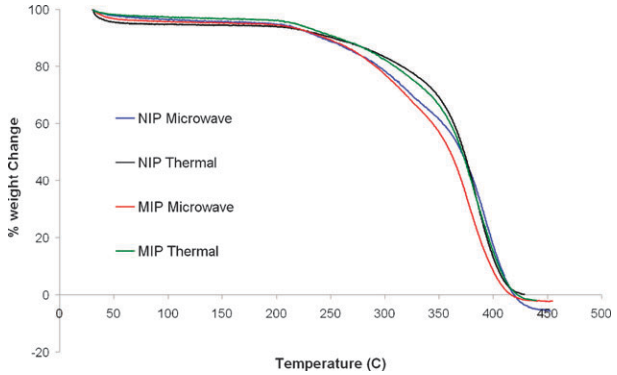

Fig. 9 Thermogravimetric analysis of polymers. Red: MIP$_{(Microwave)}$; blue: NIP$_{(Microwave)}$; green: MIP$_{(Thermal)}$; and black: NIP$_{(Thermal)}$.

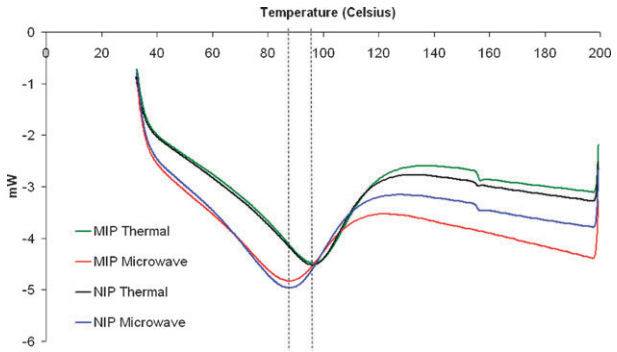

Fig. 10 Differential scanning calorimetry (DSC) trace of polymers. Red: MIP$_{(Microwave)}$; blue: NIP$_{(Microwave)}$; green: MIP$_{(Thermal)}$; and black: NIP$_{(Thermal)}$. The dotted lines show the trough minima at 88 °C for microwave polymers and 96 °C for thermal polymers. Traces are representative of duplicates.

imprinting sites. The frequency of mesoporosity is significantly greater in the thermal system, suggesting a clear relationship between porosity, polymerisation conditions and observed rebinding behaviour. Thermal imprinting is, by default, a slow and equilibrium driven process that allows the porogen and template to define the micro/mesoporous structure of the resultant polymer, leading to increased surface area, resulting in a greater number of potential binding sites (both high and low affinity) and by default, a higher binding capacity. The much faster polymerisation rates generated under microwave conditions (presumably stemming from an enhancement of polymerisation rate and auto acceleration (Trommsdorff effect),[42] reduces the influence of porogen and template on pore structure, resulting in a comparatively low surface area MIP with reduced binding capacity. With a lower comparative mesoporous surface area (to that generated by thermal imprinting) and only a modest difference in relative surface area between MIP$_{(Microwave)}$ and NIP$_{(Microwave)}$, rapid microwave polymerisation, while limiting the formation of high quality imprinting sites, appears to bestow a benefit of improved differential selectivity between high and low affinity binding sites, as reflected in the Scatchard data.

The polymers were subjected to X-Ray diffraction (XRD) and to thermal analysis by TGA and DSC. XRD showed all samples to be highly amorphous structures with no discernable differences between samples (data not shown).

TGA (Fig. 9) shows that the decomposition of the thermal polymers occurs at the higher temperature than the microwave ones, suggesting higher levels of structural cross-linking. Interestingly, both non-imprinted polymers show slightly higher thermal stability, a property that may relate to the observed differences in mesopore population, which leads to a more dense overall structure.

The DSC traces of the polymers also show distinct differences (Fig. 10), with the thermal MIP/NIP couple exhibiting higher melting points than the microwave pair (96 °C over 88 °C, respectively), a feature that is again consistent higher levels of cross-linking. The profile of the melt in all polymers is very broad suggesting a wide range of molecular weights within the samples. Interestingly, the NIP in both microwave and thermal samples appear to behave the same as the MIP, within the tolerances of the instrument (± 0.5 °C) suggesting similar composition.

Conclusions

Microwave induced bulk polymerisation of a caffeine imprinted polymer results in a 70-fold reduction in preparation time compared with conventional thermal initiation methods. The resultant MIP, while possessing similar gross morphology to its thermal counterpart, exhibits reduced binding capacity because of a comparatively small number of high affinity binding sites. The high and low affinity sites present on

$MIP_{(Microwave)}$ possessed significantly larger K_D values than their thermal counterparts, indicating poorer target recognition qualities, however the relative ratio of the these values is greater under microwave polymerisation conditions, suggesting that better discrimination between the sites exists in the case of $MIP_{(Microwave)}$. The imprint factor of $MIP_{(Microwave)}$ was found to exceed that of $MIP_{(Thermal)}$ because of comparatively lower levels of non-specific binding exhibited $NIP_{(Microwave)}$, a result stemming from the reduced surface areas of the microwave polymer couple. We speculate that the reduction in surface area is an artifact of auto acceleration processes that occur as a result of rapid polymerisation induced by microwave irradiation which limits the influence of solvent as a determinant of pore structure. Work to assess the effects of longer pre-polymer equilibration times and polymerisation time on the selectivity of microwave produced polymers is currently underway.

Materials and methods

Materials

Methacrylic acid (MAA) and ethylene glycol dimethacrylate (EGDMA) were purchased from Sigma-Aldrich (Sydney, Australia), then distilled to remove storage inhibitors. Caffeine and theophylline were purchased from Sigma-Aldrich (Sydney, Australia) and used as received. AIBN was purchased from DuPont (Melbourne, Australia) and recrystallised from acetone to remove storage inhibitors. All solvents were purchased from Sigma Aldrich and used as supplied.

Thermal polymerisation $P_{(Thermal)}$

Following a similar protocol to Theodoridis and Manesiotis,[22] caffeine (97 mg, 0.5 mmol) was dissolved in 2 mL of acetonitrile containing MAA (0.175 mL. 2 mmol) and EGDMA (1.248 mL, 6 mmol) in a 4 mL vial. AIBN (15 mg, 0.09 mmol) was then added. The sample was then degassed (N_2) for 15 min, sealed, then heated in a benchtop oven at 60 °C for 18 h. A matching non-imprinted polymer (template absent from the formulation) was prepared under identical conditions. Upon removal from the oven, the polymers were cooled, then mechanically ground using a pestle and mortar and sieved to obtain size fractions between 32 and 63 μm. Each polymer was exposed to a Soxhlet extraction of 10% acetic acid in methanol for 60 h with 2 exchanges of solvent. Finally a Soxhlet extraction of methanol only was performed for 12 h. Extract solutions were tested until no caffeine was observed to leach from the polymers. The polymers were then dried under vacuum and stored under nitrogen at room temperature.

Microwave polymerisation $P_{(Microwave)}$

Caffeine (97 mg, 0.5 mmol) was dissolved in acetonitrile (2 mL) along with MAA (0.175 mL, 2 mmol) and EGDMA (1.248 mL, 6 mmol). AIBN (15 mg, 0.09 mmol) was then added. The sample was degassed (N_2) for 15 min and sealed in a 10 mL test tube. The tube was placed in a microwave reactor (Discover Benchmate, CEM, Matthews, NC, USA) and heated at 150 W for 14 min with a maximum temperature set at 60 °C. Temperature was monitored by an infra-red thermometer, which causes the system to shut off (0 W) when the designated temperature is reached. A matching non-imprinted polymer (template molecule absent from the formulation) was prepared under the same conditions. Upon removal from the oven, the polymers were cooled, then mechanically ground using a pestle and mortar and sieved to obtain size fractions between 32 and 63 μm. Each polymer was exposed to a Soxhlet extraction of 10% acetic acid in methanol for 60 h with 2 exchanges of solvent. Finally a Soxhlet extraction of methanol only was performed for 12 h. The polymers were then dried under vacuum and stored under nitrogen at room temperature.

Solid phase extraction

An aliquot (100 mg) of each polymer was packed into a 1 mL solid phase extraction cartridge. The cartridges were then rinsed with methanol and acetone to ensure even packing and then dried under vacuum. Rebinding solutions of caffeine were prepared at the required concentrations from a 20 mmol stock solution in LC grade (Chromasolv, Sigma-Aldrich) acetonitrile. All filtration experiments were performed using a Supelco "Preppy" vacuum manifold powered by a vacuum pump. Flow rates were measured for each cartridge and the valves were adjusted to ensure equality. Total time for each volume of 1 mL was 15 s. Before loading the caffeine solution, the polymer was conditioned with 1 mL LC-grade acetonitrile. For each tube, 1 mL of the sample was loaded under vacuum and collected in the manifold in 1 ml LC vials. These samples along with a sample of the original loading concentration were sealed and analysed by HPLC. All measurements were performed in triplicate for each polymer over a range of 0.005–2 mmol. Cross-reactivity studies (substituting theophylline for caffeine), were performed in the same manner, over a 0.01–2 mmol range.

Liquid chromatography

Quantification of caffeine was achieved using a Shimadzu LC-20AD fitted with a photodiode array (PDA) SPD-M20A. A mobile phase of 50% methanol–50% water was run at 0.7 mL min^{-1} for 7 min at 29 °C, using a 150 mm × 4.6 mm 5 μm C18 reverse phase column (Econosphere, Grace Scientific, Sydney, Australia). 20 μL of sample (in acetonitrile) were injected. A calibration curve was obtained using the area of the peak appearing at t = 4.1 min (λ = 254 nm). Theophylline was analysed in an identical manner using a mobile phase of 28% methanol–72% water at 0.7 mL min^{-1} at 29 °C. Calibration curves were obtained using the area of the peak appearing at t = 5.5 min (λ = 190 nm).

Scanning electron microscopy (SEM)

Ground particles of each polymer were taken and dusted onto a carbon sticker, then coated with gold using a sputter coater (SPI, PA, USA) for 2 min (layer depth ~15–20 Å). Images were recorded using a Philips XL30 SEM fitted with an Oxford ISIS EDS.

Differential scanning calorimetry (DSC)

Approximately 2.5 mg of polymer were sealed in a crimped aluminium pan. A matching mass of aluminium silicate was

measured, sealed in a crimped pan. Both were placed on the balance within the furnace of a DSC-60 scanning calorimeter (Shimadzu, Japan). Samples were then heated from 30 °C to 200 °C at 10 °C min^{-1}, held at 200 °C for 3 min and cooled to 30 °C at the same rate.

Thermogravimetric analysis (TGA)

Approximately 5 mg of polymer were placed in an open aluminium pan. The sample was then heated at 30 °C min^{-1} from 30 °C to 600 °C using a Diamond TG/DTA (Perkin Elmer, MA, USA) and mass loss recorded.

Surface area and pore size distribution analysis

Gas adsorption analysis was carried out using a Micromeritics ASAP 2020 Accelerated Surface Area and Porosity instrument (Norcross, GA, USA). To carry out the analysis, 20–30 mg of sample were first degassed at 110 °C under vacuum for 6 h to remove any adsorbed solvent. The adsorption isotherm of this degassed sample was then measured using nitrogen as the adsorbate at a temperature of 77 K covering the partial pressure (P/P_0) range 1×10^{-6} to 1. The specific surface area of each sample was determined from the adsorption data using the linearised BET equation,[40] while the pore size distribution was calculated using a density functional theory (DFT) based approach using Micromeritics DFT Plus V2.00 software as described by Arnott *et al.*[43]

Imprinting factor

The measure of rebinding performance of a molecularly imprinted material is known as its imprinting factor (IF). This is a relative measurement of substrate rebinding against a non-imprinted reference polymer and is expressed as the ratio of bindings, $IF = [B_{MIP}]/[B_{NIP}]$.[1]

Acknowledgements

This work was funded by the Australian Research Council, The Australian Federal Police Forensic Services, and the National Insitute of Forensic Science (Australia).

References

1 C. Alexander, H. S. Andersson, L. I. Andersson, R. J. Ansell, N. Kirsch, I. A. Nicholls, J. O'Mahony and M. Whitcomb, *J. Mol. Recognit.*, 2006, **19**, 106–180.
2 A. McCluskey, C. I. Holdsworth and M. C. Bowyer, *Org. Biomol. Chem.*, 2007, **5**, 3233–3244.
3 N. W. Turner, C. W. Jeans, K. R. Brain, C. J. Allender, V. H. Hlady and D. W. Britt, *Biotechnol. Prog.*, 2006, **22**, 1474–1489.
4 A. Ellwanger, L. Karlsson, P. K. Owens, C. Berggren, C. Crecenzi, K. Ensing, S. Bayoudh, P. Cormack, D. Sherrington and B. Sellergren, *Analyst*, 2001, **126**, 784–792.
5 I. Chianella, M. Lotierzo, S. A. Piletsky, I. E. Tothill, B. Chen, K. Karim and A. P. F. Turner, *Anal. Chem.*, 2002, **74**, 1288–1293.
6 C. I. Holdsworth, M. C. Bowyer, C. Lennard and A. McCluskey, *Aust. J. Chem.*, 2005, **58**, 315–320.
7 I. A. Nicholls, H. S. Andersson, C. Charlton, H. Henschel, B. C. G. Karlsson, J. G. Karlsson, J. O'Mahony, A. M. Rosengren, K. J. Rosengren and S. Wikman, *Biosens. Bioelectron.*, 2009, **25**, 543.
8 L. J. Schwarz, M. C. Bowyer, C. I. Holdsworth and A. McCluskey, *Aust. J. Chem.*, 2006, **59**, 129–134.
9 D. Rathbone and A. Bains, *Biosens. Bioelectron.*, 2005, **20**, 1438–1442.
10 F. Puoci, F. Lemma, R. Muzzalupo, U. G. Spizzirri, S. Trombino, R. Cassano and N. Picci, *Macromol. Biosci.*, 2004, **4**, 22–26.
11 D. Wang, S. P. Hong, G. Yang and K. H. Row, *Korean J. Chem. Eng.*, 2003, **20**, 1073–1076.
12 H. Kempe and M. Kempe, *Anal. Chem.*, 2006, **78**, 3659–3666.
13 Q. Li, W. Zhangand and X. Li, *Macromol. Symp.*, 2008, **261**, 91–96.
14 S. Carter, S. Y. Lu and S. Rimmer, *Supramol. Chem.*, 2003, **15**, 213–220.
15 S. R. Carter and S. Rimmer, *Adv. Mater.*, 2002, **14**, 667–670.
16 N. Pérez, M. J. Whitcombe and E. N. Vulfson, *Macromolecules*, 2001, **34**, 830–836.
17 S. Li, S. Pilla and S. Gong, *J. Polym. Sci.*, 2009, **47**, 2352–2360.
18 F. Lanza and B. Sellergren, *Macromol. Rapid Commun.*, 2004, **25**, 59–68.
19 W. M. Mullett and E. P. C. Lai, *Anal. Chem.*, 1998, **70**, 3636–3641.
20 C. Berggren, S. Bayoudh, D. Sherrington and K. Ensing, *J. Chromatogr., A*, 2000, **889**, 105–10.
21 B. Sellergren, *TrAC, Trends Anal. Chem.*, 1999, **18**, 164–174.
22 G. Theodoridis and P. Manesiotis, *J. Chromatogr., A*, 2002, **948**, 163–169.
23 MIP-Technologies press release (online), available at http://www.miptechnologies.com/press.asp, accessed 14 August 2009.
24 G. Bunte, J. Hurttlen, H. Pontius, K. Hartlieb and H. Krause, *Anal. Chim. Acta*, 2007, **591**, 49–56.
25 K. M. Booker, M. C. Bowyer, C. I. Holdsworth and A. McCluskey, *Chem. Commun.*, 2006, 1730–1732.
26 K. M. Booker, M. C. Bowyer, C. J. Lennard, C. I. Holdsworth and A. McCluskey, *Aust. J. Chem.*, 2007, **60**, 51–56.
27 N. W. Turner, E. V. Piletska, K. Karim, M. Whitcombe, M. Malecha, Na. Magan, C. Baggiani and S. A. Piletsky, *Biosens. Bioelectron.*, 2004, **20**, 1060–1067.
28 I. A. Nicholls, *Chem. Lett.*, 1995, 1035–1036.
29 S. A. Piletsky, E. V. Piletska, K. Karim, K. W. Freebairn, C. H. Legge and A. P. F. Turner, *Macromolecules*, 2002, **35**, 7499–7504.
30 B. Hayes, *Microwave Synthesis: Chemistry at the Speed of Light*, CEM Publishing, Matthews, 2002.
31 D. Adam, *Nature*, 2003, **421**, 571–572.
32 R. Hoogenboom and U. S. Schubert, *Macromol. Rapid Commun.*, 2007, **28**, 368–386.
33 F. Wiesbrock, R. Hoogenboom and U. S. Schubert, *Macromol. Rapid Commun.*, 2004, **25**, 1739–1764.
34 C. Zhang, L. Liao and S. Gong, *Green Chem.*, 2007, **9**, 303–314.
35 L. Zong, S. Zhou, N. Sgriccia, M. C. Hawley and L. C. Kempel, *J. Microwave Power Electromagn. Energy*, 2003, **38**, 49–74.
36 D. Bogdal, P. Penczek, J. Pielichowski and A. Prociak, *Adv. Polym. Sci.*, 2003, **163**, 193–263.
37 J. Sierra, J. Palacios and E. Vivaldo-Lima, *J. Macromol. Sci., Pure Appl. Chem.*, 2006, **43**, 589–600.
38 Y. Zhang, R. Liu, Y. Hu and G. Li, *Anal. Chem.*, 2009, **81**, 967–976.
39 T. Kobayashi, Y. Murawaki, P. S. Reddy, M. Abe and N. Fujii, *Anal. Chim. Acta*, 2001, **435**, 141–149.
40 S. Brunauer, P. H. Emmett and E. Teller, *J. Am. Chem. Soc.*, 1938, **60**, 309–319.
41 N. W. Turner, N. Holmes, C. Brisbane, A. B. McGeachie, M. C. Bowyer, A. McCluskey and C. I. Holdsworth, *Soft Matter*, 2009, **5**, 3663–3671.
42 G. Odian, *Principles of Polymerization*, Wiley, New York, 2nd edn, 1981, pp. 271.
43 J. B. Arnott, R. P. Williams, A. G. Pandolfo and S. W. Donne, *J. Power Sources*, 2007, **165**, 581–590.

